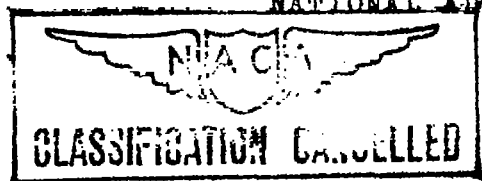


UNCLASSIFIED 3000
This document contains classified information affecting the National Defense of the United States within the meaning of the Espionage Act, US 50:81 and 82. Its transmission or the revelation of its contents in any manner to an unauthorized person is prohibited by law. Information so classified may be imparted only to persons in the military and naval Services of the United States, appropriate civilian officers and employees of the Federal Government who have a legitimate interest therein, and to United States citizens of known loyalty and discretion who of necessity must be informed thereof.

MAR 8 1941

TECHNICAL NOTES

NATIONAL ADVISORY COMMITTEE FOR AERONAUTICS



No. 796

TR 796-1-41

returned to
of the Langley
DETERMINATION OF CONTROL-SURFACE CHARACTERISTICS

FROM NACA PLAIN-FLAP AND TAB DATA

By Milton B. Ames, Jr., and Richard I. Sears
Langley Memorial Aeronautical Laboratory

FOR REFERENCE

Washington
February 1941

NOT TO BE TAKEN FROM THIS ROOM

NATIONAL ADVISORY COMMITTEE FOR AERONAUTICS

TECHNICAL NOTE NO. 796

DETERMINATION OF CONTROL-SURFACE CHARACTERISTICS

FROM NACA PLAIN-FLAP AND TAB DATA

By Milton B. Ames, Jr., and Richard I. Sears

SUMMARY

W! The data from previous NACA pressure-distribution investigations of plain flaps and tabs have been analyzed and are presented in this paper in a form readily applicable to the problems of control-surface design. The experimentally determined variation of aerodynamic parameters with flap chord and tab chord are given in chart form and comparisons are made with the theory. With the aid of these charts and the theoretical relationships for a thin airfoil, the aerodynamic characteristics for control surfaces of any plan form with plain flaps and tabs may be determined. A discussion of the basic equations of the thin-airfoil theory and the development of a number of additional equations that will be helpful in tail design are presented in the appendixes. The procedure for applying the data is described and a sample problem of tail design is included. ???

(The data presented and the method of application set forth in this report should provide a reasonably accurate and satisfactory means of computing the aerodynamic characteristics of control surfaces. ???

INTRODUCTION

The need for an improvement in the method of predicting the aerodynamic characteristics of airfoils with multiple hinged flaps, such as horizontal and vertical tail surfaces, has long been realized. A number of valuable contributions of both an experimental and a theoretical nature have been made, but the ultimate objective has not yet been attained. With the intention of more closely approaching a satisfactory solution of the problem, the National Advisory Committee for Aeronautics has undertaken a control-surface investigation.

The theoretical expressions for the lift and the pitching-moment coefficients of an airfoil and the hinge-moment coefficients of any number of flaps about any hinge position on the airfoil have been derived in references 1, 2, and 3.

Experiments have, however, failed to check the theory, especially in the cases of hinge-moment coefficients of small-chord flaps. It is for this reason that the design of tail surfaces has depended largely on experiments.

Several experimental investigations of tail surfaces have been conducted by the NACA and some recent data are presented in references 4, 5, and 6. In order to supply systematic experimental data for the aerodynamic and the structural design of control surfaces, a pressure-distribution investigation of the section characteristics of an NACA 0009 airfoil with various sizes of plain flaps and tabs was conducted. The results are reported in references 7, 8, and 9.

In order to make the data of references 7, 8, and 9 more readily applicable for design purposes, curves have been prepared to give experimental parameters for a wide range of flap and tab chords. The parameters given in this paper may be used with the expressions presented in references 1, 2, and 3 to determine the aerodynamic characteristics of tail surfaces with plain flaps and tabs.

SYMBOLS

The coefficients and the symbols used in the theoretical discussion are defined as follows:

$$c_n = \frac{n}{qc}$$

$$C_N = \frac{N}{qS}$$

$$c_m = \frac{m}{qc^2}$$

$$C_m = \frac{M}{qc^2b}$$

$$c_{h_f} = \frac{h_f}{q c_f a}$$

$$C_{h_f} = \frac{H_f}{q c_f a b_f}$$

$$c_{h_t} = \frac{h_t}{q c_t a}$$

$$C_{h_t} = \frac{H_t}{q c_t a b_t}$$

where c_n airfoil section normal-force coefficient
 C_N airfoil normal-force coefficient
 c_m airfoil section pitching-moment coefficient about quarter-chord point of airfoil
 C_m airfoil pitching-moment coefficient about quarter-chord point of airfoil
 c_{h_f} flap section hinge-moment coefficient
 C_{h_f} flap hinge-moment coefficient
 c_{h_t} tab section hinge-moment coefficient
 C_{h_t} tab hinge-moment coefficient
 n section normal force of airfoil
 N normal force of airfoil
 m section pitching moment of airfoil about quarter-chord point
 M pitching moment of airfoil about quarter-chord point
 h_f flap section hinge moment
 H_f flap hinge moment

h_t	tab section hinge moment
H_t	tab hinge moment
q	dynamic pressure
c	mean geometric chord of basic airfoil with flap and tab neutral
\overline{c}	root mean square airfoil chord
c_f	mean geometric flap chord
\overline{c}_f	root mean square flap chord
c_t	mean geometric tab chord
\overline{c}_t	root mean square tab chord
S	airfoil area
b	airfoil span
b_f	flap span
b_t	tab span
α	angle of attack
α_0	angle of attack from zero lift for airfoil of infinite aspect ratio with flap and tab neutral
α_a	angle of attack from zero lift for finite airfoil with flap and tab neutral
δ_f	flap deflection with respect to airfoil
δ_t	tab deflection with respect to flap
A	aspect ratio

DISCUSSION

Equations

The theory of thin airfoils is developed in refer-

ence 1 and is extended to include a hinged plain flap in reference 2. The derivations, completed in reference 3, give the theoretical relationships for a finite airfoil with a multiple hinged plain-flap system. The general theory, in agreement with experiment, indicates a linear variation of angle of attack, flap deflection, pitching-moment coefficient and hinge-moment coefficient with lift coefficient. In order to simplify the analysis, several assumptions were made in developing the theory, two of the more important being that the airfoil may be replaced by a mean camber line and that the fluid flow leaves the trailing edge of the airfoil smoothly. The aerodynamic characteristics of an airfoil with a plain flap are expressed in terms of theoretically determined parameters (see figs. 1 and 2), which are used in the equations for the airfoil and the flap coefficients. These parameters are identified and transformed into the partial differentials of standard NACA coefficients in appendix A. Because a conventional control surface is essentially an airfoil with a series of plain flaps, these airfoil equations may be applied to determine the characteristics of control surfaces. The equations in standard NACA form are:

$$C_N = \left(\frac{\partial C_N}{\partial \alpha} \right)_{\delta_f, \delta_t} \left[\alpha_a - \left(\frac{\partial \alpha}{\partial \delta_f} \right)_{c_n, \delta_t} \delta_f - \left(\frac{\partial \alpha}{\partial \delta_t} \right)_{c_n, \delta_f} \delta_t \right] \quad (1)$$

$$C_m = \left(\frac{\partial C_m}{\partial c_n} \right)_{\delta_f, \delta_t} C_N + \left(\frac{\partial C_m}{\partial \delta_f} \right)_{c_n, \delta_t} \delta_f + \left(\frac{\partial C_m}{\partial \delta_t} \right)_{c_n, \delta_f} \delta_t \quad (2)$$

$$C_{h_f} = \left(\frac{\partial C_{h_f}}{\partial c_n} \right)_{\delta_f, \delta_t} C_N + \left(\frac{\partial C_{h_f}}{\partial \delta_f} \right)_{c_n, \delta_t} \delta_f + \left(\frac{\partial C_{h_f}}{\partial \delta_t} \right)_{c_n, \delta_f} \delta_t \quad (3)$$

$$C_{h_f} = \left(\frac{\partial C_{h_f}}{\partial \alpha} \right)_{\delta_f, \delta_t} \alpha_a + \left(\frac{\partial C_{h_f}}{\partial \delta_f} \right)_{\alpha, \delta_t} \delta_f + \left(\frac{\partial C_{h_f}}{\partial \delta_t} \right)_{\alpha, \delta_f} \delta_t \quad (4)$$

The subscripts indicate the factors that are held constant when the partial derivatives are taken.

The relationships in equations (1), (2), and (3) readily lend themselves to the prediction of control-surface characteristics, such as tab and flap setting for trim, tab operation as a balance, and the parameters for free-control stability. From the basic relations, some

of the equations for determining the control characteristics are developed in appendix B. If C_N is the normal-force coefficient of the tail required for equilibrium, the tab deflection to trim with zero control force is:

$$\delta_t(C_{hf}=0) = \frac{C_N(C_{hf}=0) \left[-\frac{1}{\left(\frac{\partial C_N}{\partial \alpha}\right)_{\delta_f, \delta_t} \left(\frac{\partial \alpha}{\partial \delta_f}\right)_{c_n, \delta_t}} + \frac{\left(\frac{\partial C_{hf}}{\partial c_n}\right)_{\delta_f, \delta_t}}{\left(\frac{\partial C_{hf}}{\partial \delta_f}\right)_{c_n, \delta_t}} \right] + \frac{\alpha_a}{\left(\frac{\partial \alpha}{\partial \delta_f}\right)_{c_n, \delta_t}}}{\frac{\left(\frac{\partial \alpha}{\partial \delta_t}\right)_{c_n, \delta_f}}{\left(\frac{\partial \alpha}{\partial \delta_f}\right)_{c_n, \delta_t}} - \frac{\left(\frac{\partial C_{hf}}{\partial \delta_t}\right)_{c_n, \delta_f}}{\left(\frac{\partial C_{hf}}{\partial \delta_f}\right)_{c_n, \delta_t}}} \quad (5)$$

and the corresponding flap deflection is

$$\delta_f(C_{hf}=0) = -\frac{1}{\left(\frac{\partial \alpha}{\partial \delta_f}\right)_{c_n, \delta_t}} \left[\frac{C_N(C_{hf}=0)}{\left(\frac{\partial C_N}{\partial \alpha}\right)_{\delta_f, \delta_t}} - \alpha_a + \left(\frac{\partial \alpha}{\partial \delta_t}\right)_{c_n, \delta_f} \delta_t(C_{hf}=0) \right] \quad (6)$$

If the control surface is equipped with a balancing tab, where $\delta_t = K\delta_f + \delta_{t_0}$, and δ_{t_0} is the initial tab deflection for trim and K is the rate of change of the tab deflection with the flap deflection, then at any angle of attack the flap deflection for zero hinge-moment coefficient (free-floating angle) is

$$\delta_f (c_{hf}=0) = \left[\begin{array}{c} \left(\frac{\partial c_{hf}}{\partial c_n} \right) \delta_f, \delta_t \left(\frac{\partial c_N}{\partial \alpha} \right) \delta_f, \delta_t \left[- \left(\frac{\partial c_{hf}}{\partial c_n} \right) \alpha_a + \left(\frac{\partial c_{hf}}{\partial c_n} \right) \left(\frac{\partial c_N}{\partial \alpha} \right) \left(\frac{\partial \alpha}{\partial \delta t} \right) c_n, \delta_f \right] \delta t_0 \\ - \left(\frac{\partial c_{hf}}{\partial c_n} \right) \left(\frac{\partial c_N}{\partial \alpha} \right) \delta_f, \delta_t \left(\frac{\partial \alpha}{\partial \delta f} \right) c_n, \delta_t + K \left[- \left(\frac{\partial c_{hf}}{\partial c_n} \right) \delta_f, \delta_t \left(\frac{\partial c_N}{\partial \alpha} \right) \left(\frac{\partial \alpha}{\partial \delta t} \right) c_n, \delta_f + \left(\frac{\partial c_{hf}}{\partial \delta t} \right) c_n, \delta_f \right] \end{array} \right] \quad (7)$$

and the corresponding normal-force coefficient is

$$c_N (c_{hf}=0) = \left(\frac{\partial c_N}{\partial \alpha} \right) \delta_f, \delta_t \left[\alpha_a - \left(\frac{\partial \alpha}{\partial \delta f} \right) \delta_f (c_{hf}=0) - \left(\frac{\partial \alpha}{\partial \delta t} \right) c_n, \delta_f \left(K \delta_f (c_{hf}=0) + \delta t_0 \right) \right] \quad (8)$$

The following parameters, developed in appendix B, are of particular importance for calculations of free-control stability.

$$\begin{aligned} \left(\frac{\partial \delta f}{\partial \alpha} \right) c_{hf=0} &= \left(\frac{\partial c_{hf}}{\partial c_n} \right) \delta_f, \delta_t \left(\frac{\partial c_N}{\partial \alpha} \right) \delta_f, \delta_t \left(\frac{\partial c_N}{\partial \alpha} \right) \delta_f, \delta_t \\ &= - \left(\frac{\partial c_{hf}}{\partial c_n} \right) \delta_f, \delta_t \left(\frac{\partial c_N}{\partial \alpha} \right) \delta_f, \delta_t \left(\frac{\partial \alpha}{\partial \delta f} \right) c_n, \delta_t + \left(\frac{\partial c_{hf}}{\partial c_n} \right) \delta_f, \delta_t \left[- \left(\frac{\partial c_{hf}}{\partial c_n} \right) \delta_f, \delta_t \left(\frac{\partial c_N}{\partial \alpha} \right) \left(\frac{\partial \alpha}{\partial \delta t} \right) c_n, \delta_f + \left(\frac{\partial c_{hf}}{\partial \delta t} \right) c_n, \delta_f \right] \quad (9) \\ \left(\frac{\partial c_N}{\partial \alpha} \right) c_{hf=0} &= \left(\frac{\partial c_N}{\partial \alpha} \right) \delta_f, \delta_t \left\{ 1 - \left[\left(\frac{\partial \alpha}{\partial \delta f} \right) c_n, \delta_t + K \left(\frac{\partial \alpha}{\partial \delta t} \right) c_n, \delta_f \right] \left(\frac{\partial \delta f}{\partial \alpha} \right) c_{hf=0} \right\} \quad (10) \end{aligned}$$

The experimental values of the parameters in the foregoing equations are presented in the following section. Although some of the equations may appear cumbersome, it is believed that the form used is most easily applicable to the practical design of a control surface. From theoretical considerations, however, these relationships may be much more easily understood if the various factors are combined into other parameters as shown in appendix B.

Experimental Data

Aerodynamic parameters.--Experimental curves (figs. 1 and 2) have been prepared for use in determining the aerodynamic characteristics of any control surface with a plain-flap aileron, elevator, or rudder with sealed gaps. These curves, to be used in conjunction with the equations in the preceding section, are plots giving the variation of aerodynamic parameters with the ratio of flap chord to airfoil chord. The parameters, obtained for the NACA 0009 airfoil from an analysis of the section data presented in references 7, 8, and 9, are chosen to be independent of aspect ratio. The theoretical curves developed by Glauert and Perring (references 2 and 3) for the thin airfoil are reproduced in figures 1 and 2 for comparison.

From an analysis of the data in references 7, 8, and 9, it was possible to define all of the experimental curves of figures 1 and 2 except in figure 2(c) by points at c_f/c of 0, 0.03, 0.05, 0.06, 0.08, 0.09, 0.10, 0.15, 0.16, 0.24, 0.30, 0.50, 0.80, and 1.00. The experimental curves of figure 2(c) are defined by points at values of c_f/c of 0.30, 0.50, 0.80, and 1.00 for the tab sizes of $0.10c_f$ and $0.30c_f$ and at $0.30c_f/c$, $0.50c_f/c$, and $0.80c_f/c$ for the $0.20c_f$ tab size. The curve for the $0.20c_f$ tab was, however, extrapolated for values of c_f/c from 0.80 to 1.00. For all the parameters of these two figures it was possible to fair the curves with practically no dispersion of points.

In figures 1 and 2 the experimental curves have the same general shape as the theoretical curves derived in references 1, 2, and 3, although in most cases their magnitudes are somewhat less. The poorest agreement was

found in the curves of $\left(\frac{\partial c_{hf}}{\partial \delta_f}\right)_{c_n, \delta_t}$ and $\left(\frac{\partial c_{hf}}{\partial \delta_t}\right)_{c_n, \delta_f}$

in figures 2(a) and 2(c), where the theoretical slopes for small-chord flaps were much higher negatively than those given by experiment. This discrepancy has been observed in other comparisons between theory and experiment. Because the theoretical parameters were determined on the assumption of a continuous flow of a perfect, nonviscous fluid, an assumption that is not valid under actual conditions, the disagreement might be expected. The discrepancy between theory and experiment is important because it occurs within the c_f/c range in which most control-surface flaps and tabs lie. The portion of the hinge-moment coefficient attributed to the effective camber

$\left(\frac{\partial c_{h_f}}{\partial \delta_f}\right)_{c_n, \delta_t} \delta_f$ (fig. 2(a)) is generally many times

greater than the portion caused by the circulation

$\left(\frac{\partial c_{h_f}}{\partial c_n}\right)_{\delta_f, \delta_t} C_N$ (fig. 2(b)).

A comparison between figures 2(a) and 2(c) indicates that, for tab sizes greater than $0.10c_f$, the flap hinge-moment coefficient obtained by deflecting the tab a given amount is greater than that obtained by deflecting the flap the same amount. This result agrees with other test data (reference 10) and indicates that a full-span balancing tab, with a chord greater than $0.10c_f$ and a 1:1 ratio of tab deflection to flap deflection, will produce overbalance.

From the test results of an NACA 0009 airfoil reported in references 7, 8, and 9, it was also experimentally determined that $\left(\frac{\partial c_n}{\partial \alpha}\right)_{\delta_f, \delta_t} = 0.095$ and $\left(\frac{\partial c_m}{\partial c_n}\right)_{\delta_f, \delta_t} = -0.0105$.

Allowable flap and tab deflections.— Because the relationships in equations (1), (2), (3), and (4) are true only for the condition of a linear variation of the aerodynamic coefficients, it is necessary to determine for various angles of attack the maximum deflection of a flap for the linear variation of the lift. In order to obtain the minimum control force for a given maximum lift with a plain flap, it is generally better to operate the flap

within this linear range than to use a smaller chord flap that must operate at flap deflections beyond the linear range to give the required lift.

The approximate maximum allowable flap deflection for linear limits of airfoil characteristics at several angles of attack are plotted against the ratio of flap chord to airfoil chord in figure 3. These limits of maximum flap deflection, obtained by experiment from the data of references 7, 8, and 9 for infinite aspect ratio at an effective Reynolds number of 3,410,000, are the approximate angles at which the variation of c_n with δ_f ceases to be linear. In most cases, however, the limits do not indicate the flap stall because the stall was observed to occur generally at a flap deflection from 2° to 5° greater. In some cases, when the tab was deflected in the direction opposite to the flap, the change from the linear variation and also the stall were delayed. The broken portions of the curves of figure 3 indicate that, because of the irregular flow over the small-chord flaps, some uncertainty exists as to the limits of the linear variation of the characteristic slopes in this region.

The flap-deflection limits for any given control surface of finite span are dependent upon the aspect ratio, the plan form, the twist, and the scale effect. Generally, an increase in scale would tend to increase the maximum allowable angle of attack and the flap deflection. Various free-flight tests have shown, however, that for critical conditions the stalls, and hence the limits of the linear variation of the aerodynamic characteristics, may not necessarily occur in flight in the same order that the tunnel tests have indicated. Because the limits presented in figure 3 are generally several degrees below the stall obtained by the experiments of references 7, 8, and 9 and because most control surfaces will be at a larger scale than the scale of these experiments, it is reasonable to assume that the limits are conservative.

If the scale effect is neglected, the limits may be determined by computing the local angles of attack at the critical section for various flap deflections by the method of reference 11. These angles of attack can then be plotted against the flap deflection to find the intersection with the allowable-limit curve for infinite aspect ratio. For all practical purposes the limits for the flap deflection and the angle of attack, when the lift is small, may be assumed to be the same for any aspect ratio.

This assumption is justifiable because the magnitude of the correction lies within the limits of the experimental accuracy in determining the curves for infinite aspect ratio.

Experiments (references 7 to 10) indicate that tab effectiveness decreases with an increase in the flap deflection. There is reason to believe, however, that on conventional finite control surfaces a satisfactory maximum for tab deflection exists between the angles of $\pm 15^\circ$ and $\pm 20^\circ$ for moderate flap deflections. This result would indicate that, for a constant tab chord, it is better to use a large-span tab deflected to a small angle than a short-span tab deflected to a large angle.

Effect of Aspect Ratio

The slope of the normal-force curve $\partial C_N / \partial \alpha$ in equation (1) for a finite airfoil is dependent on aspect ratio A and may be corrected in the following manner:

$$\left(\frac{\partial C_N}{\partial \alpha} \right)_{\delta_f, \delta_t} = p \frac{\left(\frac{\partial c_n}{\partial \alpha} \right)_{\delta_f, \delta_t}}{1 + \frac{57.3r \left(\frac{\partial c_n}{\partial \alpha} \right)_{\delta_f, \delta_t}}{\pi A}} \quad (11)$$

where $\partial c_n / \partial \alpha$ is the slope of the normal-force curve, per degree, for infinite aspect ratio. The term p is a correction factor for small aspect ratios, and values obtained from unpublished data are used in figure 4. For horizontal surfaces with end plates, such as twin vertical surfaces, the value of p is 1. The factor r , a correction for end-plate effect due to twin vertical surfaces, was obtained from reference 4, and its values are reproduced in figure 4. For horizontal surfaces with single vertical surfaces, the value of r is 1. Because the parameters

$\left(\frac{\partial \alpha}{\partial \delta_f} \right)_{c_n, \delta_t}$ and $\left(\frac{\partial \alpha}{\partial \delta_t} \right)_{c_n, \delta_f}$ in equation (1) involve no

change in circulation, they are unaffected by aspect ratio.

In equation (2), if the pitching-moment coefficient is taken about the aerodynamic center of the airfoil and

designated $C_{ma.c.}$, the parameter $\left(\frac{\partial C_{ma.c.}}{\partial C_N}\right)_{\delta_f, \delta_t}$ is equal to zero because

$$\left(\frac{\partial C_{ma.c.}}{\partial C_N}\right)_{\delta_f, \delta_t} = \frac{\left(\frac{\partial C_{ma.c.}}{\partial \alpha}\right)_{\delta_f, \delta_t}}{\left(\frac{\partial C_N}{\partial \alpha}\right)_{\delta_f, \delta_t}}$$

where by definition $\left(\frac{\partial C_{ma.c.}}{\partial \alpha}\right)_{\delta_f, \delta_t}$ is equal to zero.

The same statement is substantially true when the pitching-moment coefficients are determined about the quarter-chord point of the airfoil because the values of the parameter are so small that, in most cases, they may be neglected. The other parameters in both this equation and in equation (3) are unaffected by the aspect ratio because they were determined for a condition of constant circulation (C_N held constant). Thus, it should be evident that the variation of equations (2) and (3) with the aspect ratio depends only upon the corrected value of C_N for the finite airfoil as determined in equation (1).

All the parameters in equation (4) are affected by the aspect ratio. The slope $\left(\frac{\partial C_{hf}}{\partial \alpha}\right)_{\delta_f, \delta_t}$ may be corrected in the same manner as $\left(\frac{\partial C_N}{\partial \alpha}\right)_{\delta_f, \delta_t}$, but the slopes c of $\left(\frac{\partial C_{hf}}{\partial \delta_f}\right)_{\alpha, \delta_t}$ and $\left(\frac{\partial C_{hf}}{\partial \delta_t}\right)_{\alpha, \delta_f}$ vary in a more complex manner. It can be shown that

$$\left(\frac{\partial C_{hf}}{\partial \delta_f}\right)_{\alpha, \delta_t} = -\left(\frac{\partial C_{hf}}{\partial \alpha}\right)_{\delta_f, \delta_t} \left(\frac{\partial \alpha}{\partial \delta_f}\right)_{C_N, \delta_t} + \left(\frac{\partial C_{hf}}{\partial \delta_f}\right)_{C_N, \delta_t}$$

From this relation it may be noted that the parameters

$$\left(\frac{\partial \alpha}{\partial \delta_f}\right)_{C_N, \delta_t} \text{ and } \left(\frac{\partial C_{hf}}{\partial \delta_f}\right)_{C_N, \delta_t} \text{ will not be affected by}$$

changes in aspect ratio because the parameters were determined for a condition of constant circulation. The value

of $\left(\frac{\partial C_{hf}}{\partial \alpha}\right)_{\delta_f, \delta_t}$ must, however, be corrected for aspect

ratio as previously mentioned. Hence, the value of the parameter $\left(\frac{\partial C_{hf}}{\partial \delta_f}\right)_{\alpha, \delta_t}$ may be corrected for aspect ratio

by correcting only the portion of the expression containing the parameter $\left(\frac{\partial C_{hf}}{\partial \alpha}\right)_{\delta_f, \delta_t}$. In a similar manner,

the parameter $\left(\frac{\partial C_{hf}}{\partial \delta_t}\right)_{\alpha, \delta_f}$ must also be corrected for aspect ratio.

The results of model tests and flight tests are generally presented in a form from which the parameters in equation (4) may be obtained. Because the parameters in equation (4) are affected by changes in aspect ratio, the experimental parameters for hinge-moment coefficients presented in this report are given in the form suitable for use in equation (3), so that they may be used for any aspect ratio.

Effect of Plan Form

Because all the parameters of figures 1 and 2 are independent of normal induced velocity, they are independent of plan form and twist as well as of aspect ratio. In general, in order to compute the characteristics of any finite control surface, it is necessary to compute the spanwise lift distribution for each flight condition as indicated in reference 11. For the special case of a control surface having an elliptical span-load curve, the aerodynamic parameters can be computed in the manner to be indicated. Such a surface will be one of elliptical chord distribution and of constant ratio of flap to airfoil chord. If for practical purposes the assumption is made that, for any control surface, elliptical lift distribution is approximated, the aerodynamic characteristics may be readily estimated by using the experimental data in figures 1, 2, 3, and 4 in the following manner:

- (1) Determine the ratios of c_f/c and c_t/c at as many stations as may be necessary to define the surfaces.
- (2) Obtain the values for the slopes at each station from figures 1 and 2 and plot them against the span. In order to sum up properly the parameters $\left(\frac{\partial c_{hf}}{\partial c_n}\right)_{\delta_f, \delta_t}$, $\left(\frac{\partial c_{hf}}{\partial \delta_f}\right)_{c_n, \delta_t}$, and $\left(\frac{\partial c_{hf}}{\partial \delta_t}\right)_{c_n, \delta_f}$, it is essential that they be based upon a common chord. Therefore, multiply the slopes obtained from figure 2 by the square of the ratio of the flap chord at the station in question to the root-mean-square flap chord $(c_f/\bar{c}_f)^2$ and plot the product.
- (3) Integrate the curves and divide by the total airfoil span, thus obtaining the effective parameter for the entire control surface.
- (4) For partial-span tabs it is necessary to introduce an additional factor to allow for the effect of the normal velocities induced over the rest of the wing by the tab. Because the value of this factor has not yet been satisfactorily determined for a general case, it must be neglected at present.

APPLICATION OF DATA TO HORIZONTAL TAILS

Inasmuch as the determination of the proper horizontal and vertical tail areas, where stability is the main consideration, is beyond the scope of this report, only the general problems involved in obtaining adequate control will be considered. The equations and the charts already presented readily lend themselves to the solution of the problems.

The elevator size is usually determined by the requirements of landing the airplane because getting the tail down in the presence of the ground is generally the most critical condition. This discussion and the sample

problem of tail design included will therefore be devoted mainly to the determination of the elevator required for landing and to the characteristics of the tail.

Before calculations can be made, however, certain characteristics of the airplane must be known: namely, the pitching-moment coefficient, the angle of downwash, and the dynamic pressure in the region of the tail. These quantities should preferably come from wind-tunnel tests of the model in question because nacelle fairings and interference effects are critical. The effects of the slipstream or of a windmilling propeller should not be neglected. If wind-tunnel tests are lacking, the characteristics may be roughly computed from other test data, such as those given in reference 12.

Because the presence of the ground affects the downwash and the dynamic pressure over the tail in a manner that has not yet been satisfactorily determined, horizontal-tail designs must be based on assumptions rather than be put on a rational basis. Until further investigation sets forth either a method of calculating the ground effect or a tunnel technique for measuring it, the assumption can be made that, during a landing, the angle of downwash at the tail is approximately zero.

In order to illustrate the method of application of the data, an example is presented for an airplane having the dimensions given in the following table.

(The primed values refer to horizontal-tail characteristics)

Definition	Dimension
Tail length from most forward center-of-gravity location of airplane to quarter-chord point of horizontal tail surface----	$l = 20.0 \text{ ft}$
Mean aerodynamic chord of wing-----	$c_w = 6.8 \text{ ft}$
Wing area-----	$S = 236 \text{ sq ft}$
Tail area-----	$S' = 48 \text{ sq ft}$
Tail span-----	$b' = 12.8 \text{ ft}$
Root mean square chord of tail-----	$\bar{c}' = 3.75 \text{ ft}$
Aspect ratio of tail-----	$A' = 3.4$
Height of quarter-chord point of horizontal tail above the ground (landing)-----	$d_g' = 3.75 \text{ ft}$
Height of horizontal tail above center of gravity of airplane measured normal to tail chord-----	$d' = 2 \text{ ft}$
Angle of attack of airplane (landing)-----	$\alpha = 14.2^\circ$
Angle of incidence of horizontal tail-----	$i' = 2.0^\circ$
Assumed ratio of tab chord to horizontal-tail chord-----	$c_t'/c' = 0.06$
Maximum tab deflection-----	$\delta_{t \text{ max}}' = 15^\circ$
Stick length-----	$s = 1.75 \text{ ft}$
Maximum deflection of control stick when deflecting the elevator-----	$\delta_s' = \pm 30^\circ$
Pitching-moment coefficient about center of gravity of model without tail ($\alpha = 14.2^\circ$)-----	$C_{m_{c.g.}} = -0.135$
Angle of downwash at tail (assumed to have been determined from wind-tunnel tests)---	$\epsilon = 2.2^\circ$
Ratio of average dynamic pressure over tail to dynamic pressure of free air stream---	$\bar{q}'/q = 0.96$

Elevator Chord

The process of calculating the elevator chord required to land the airplane is as follows:

- (1) Compute the effective aspect ratio A_e' of the tail surface in the presence of the ground. From reference 13, when applied to a horizontal tail surface,

$$A_e' = \frac{A'}{1 - \sigma} \quad (12)$$

where between the limits

$$\frac{1}{15} < \frac{d_g'}{b'/2} < \frac{1}{2}$$

$$\sigma = \frac{1 - 0.66 \left(\frac{d_g'}{b'/2} \right)}{1.05 + 3.7 \left(\frac{d_g'}{b'/2} \right)} \quad (13)$$

For the example,

$$\frac{d_g'}{b'/2} = \frac{3.75}{6.4} = 0.586$$

Therefore

$$\sigma = \frac{1 - 0.66(0.586)}{1.05 + 3.7(0.586)} = 0.191$$

and

$$A_e' = \frac{3.4}{1 - 0.191} = 4.2$$

- (2) Compute the slope of the lift curve of the horizontal tail by equation (11) as already outlined. From figure 4, $p = 0.933$ and $r = 1$

and, from reference 8, for an NACA 0009 airfoil, $\partial c_n / \partial \alpha$ is 0.095.

Therefore

$$\left(\frac{\partial c_N}{\partial \alpha} \right)_{\delta_f, \delta_t} = \frac{0.933 (0.095)}{1 + \frac{57.3 (0.095)}{\pi 4.2}} = 0.063$$

- (3) Determine the angle of attack of the horizontal tail surface:

$$\begin{aligned} \alpha_a' &= \alpha + i' - \epsilon \\ &= 14.2^\circ + 2.0^\circ - 2.2^\circ \\ &= 14.0^\circ \end{aligned}$$

- (4) Approximate the pitching-moment coefficient of the tail C_m' by assuming a ratio of c_f'/c' and substituting in equation (2), using the maximum values of δ_f and δ_t . Obtain the value of $\delta_f'_{\max}$ from figure 3.

If, for this example, c_f'/c' is estimated to be 0.35, then from the experimental curve in figure 1(a),

$$\left(\frac{\partial c_m}{\partial \delta_f} \right)_{c_n, \delta_t} = -0.0090$$

From figure 3, if it is assumed that $\alpha_a' \hat{=} \alpha_0'$ at $\alpha_0' = 14^\circ$, then $\delta_f'_{\max} = -25.6^\circ$.

From equation (2), it is estimated that $C_N' = -0.2$ and assumed that for a tab with dimensions of 0.3 b' by 0.06 c' ,

$$\begin{aligned} \left(\frac{\partial c_m}{\partial \delta_t} \right)_{c_n, \delta_f} &= 0.3 (-0.0050) \\ &= -0.0015 \end{aligned}$$

Therefore

$$C_m' = (-0.0105)(-0.2) + (-0.0090)(-25.6) + (-0.0015)(15) \\ = 0.21$$

- (5) Estimate the chord-force coefficient of the tail C_c' from the curves in reference 4. The omission of this term will, however, have no great effect on the results.

From figure 5, reference 4,

$$C_c' = 0.25 \text{ (approx.)}$$

- (6) Calculate the normal-force coefficient of the tail required to maintain equilibrium by the equation

$$C_N' = \frac{1}{l} \left(\frac{q}{q_1} \frac{S}{S_1} C_{m.c.g.} c_w + C_m' \bar{c}' + C_c' d' \right) \quad (14) \\ = \frac{1}{20.0} \left[\left(\frac{1}{0.96} \right) \left(\frac{236}{48} \right) (-0.135)(6.8) + (0.21)(3.75) + 2(0.25) \right] \\ = -0.17$$

- (7) From equation (1), compute the product

$$\left(\frac{\partial \alpha}{\partial \delta_f} \right)_{c_n, \delta_t} \delta_f' = - \frac{C_N'}{\left(\frac{\partial C_N}{\partial \alpha} \right)_{\delta_f, \delta_t}} + \alpha_a' + \left(\frac{\partial \alpha}{\partial \delta_t} \right)_{c_n, \delta_f} \delta_t' \quad (15)$$

For the example cited, $\left(\frac{\partial \alpha}{\partial \delta_t} \right)_{c_n, \delta_f}$ is approximated to be

$$(0.3)(-0.20) = -0.06$$

Thus, with $\delta_t'_{\max} = 15^\circ$,

$$\left(\frac{\partial \alpha}{\partial \delta_f} \right)_{c_n, \delta_t} \delta_f' = - \frac{-0.17}{0.063} + 14.0 - (-0.06)(15) \\ = 17.6^\circ$$

If accurate downwash measurements are lacking but adequate wind-tunnel data are available, it would be a better procedure to modify steps (4) to (7) in the following manner. Obtain by experiment the pitching-moment coefficient of the model, including the tail undivided into stabilizer and elevator. Then calculate the increments of chord-force and pitching-moment coefficients of the tail about its quarter-chord point to obtain the increment of normal-force coefficient necessary to balance the airplane. The subscript f with C_N' , C_m' , and C_c' refers to the change caused by the flap (elevator) deflection.

$$C_{N_f}' = \frac{1}{l} \left(\frac{q}{q'} \frac{S}{S'} C_{m_{f.c.g.}} c_w + C_{m_f}' \bar{c}' + C_{c_f}' d' \right)$$

The product $\left(\frac{\partial \alpha}{\partial \delta_f} \right)_{c_n, \delta_t} \delta_f'$ is obtained:

$$\left(\frac{\partial \alpha}{\partial \delta_f} \right)_{c_n, \delta_f} \delta_f' = - \left(\frac{C_{N_f}'}{\frac{\partial C_N}{\partial \alpha}} \right) - \left(\frac{\partial \alpha}{\partial \delta_t} \right)_{c_n, \delta_t} \delta_t' \quad (16)$$

From this point on, the procedure is the same as before. This method has the advantage that, although it is still necessary to calculate the angle of attack of the tail (and hence the downwash) to determine the maximum flap deflection, the downwash computation does not enter

into the calculations for the product $\left(\frac{\partial \alpha}{\partial \delta_f} \right)_{c_n, \delta_t} \delta_f'$

and hence possible inaccuracies are minimized.

- (8) Assign convenient values of δ_f' and compute from the product of equation (15) values of

$\left(\frac{\partial \alpha}{\partial \delta_f} \right)_{c_n, \delta_t}$ Obtain from figure 1(b) the

values of c_f'/c' corresponding to the computed

values of $\left(\frac{\partial \alpha}{\partial \delta_f} \right)_{c_n, \delta_t}$ and plot them against

the assigned δ_f' values.

For the example cited, table I lists the computed values of $\left(\frac{\partial \alpha}{\partial \delta_f}\right)_{c_n, \delta_t}$ and the values of c_f'/c' that correspond to the assigned values of δ_f' when $\delta_t' = 15^\circ$.

TABLE I

δ_f' (deg)	$\left(\frac{\partial \alpha}{\partial \delta_f}\right)_{c_n, \delta_t}$	c_f'/c'
-18.4	-0.960	0.800
-20.0	-.880	.647
-25.0	-.705	.430
-30.0	-.587	.315
-35.0	-.503	.241
-40.0	-.441	.192

The values given in table I are plotted in figure 5. This curve represents the deflection of each flap size required to produce the required normal-force coefficient C_N' at the given angle of attack. This procedure was repeated at $\delta_t = 0^\circ$. The results are likewise plotted in figure 5.

- (9) Plot the curve of maximum allowable δ_f' against values of c_f'/c' as obtained from figure 3 for the required angle of attack of the tail surface. This curve is also plotted in figure 5. The intersection of these curves will indicate the minimum effective flap-chord ratio c_f'/c' and the flap deflection necessary to obtain the required C_N' of the tail at the angle of attack for landing. The mean value of $\left(\frac{\partial \alpha}{\partial \delta_f}\right)_{c_n, \delta_t}$ for the entire tail

surface should be that corresponding to this flap-chord ratio c_f'/c' .

From a consideration of the maximum free-control stability and the lowest control forces, it

It is apparent that this flap (elevator) of the minimum allowable size should be the optimum size. Hence, for the example cited, the curves of figure 5 intersect at $\delta_f' = -26^\circ$ (approx.), $c_f'/c' = 0.40$. This result corresponds to an effective $\left(\frac{\partial \alpha}{\partial \delta_f}\right)_{c_n, \delta_t} = -0.67$ (fig. 1(b)).

The plan form and the total area having already been tentatively determined, the object now is to divide the tail surface into stabilizer and elevator in such manner as to give a mean

value of $\left(\frac{\partial \alpha}{\partial \delta_f}\right)_{c_n, \delta_t}$ corresponding to the

effective flap-chord ratio just computed. This division must of necessity be done by a method of successive approximations in locating the hinge axis or in making alterations to the plan form. The procedure for determining the effective value of any of the parameters has already been indicated. The proper location of the hinge axis having been esti-

mated, the effective parameter $\left(\frac{\partial \alpha}{\partial \delta_f}\right)_{c_n, \delta_t}$ of the assumed arrangement can be found.

When the hinge line is properly estimated, the effective $\left(\frac{\partial \alpha}{\partial \delta_f}\right)_{c_n, \delta_t}$ thus obtained should

be the same as the value previously calculated. If it is smaller, the flap size will not satisfy the design requirements; if it is larger, the stick force may be greater, as can be seen from the stick-force curve for a rectangular tail in figure 6. Likewise, the free-control stability will be decreased.

For the example cited, with the plan form of the tail assumed to be that indicated in figure 7, the hinge line has been located on the second approximation. A constant flap chord up to

the tip section has been chosen because it can be shown that, in general, such a flap will have lower stick forces than one having a highly tapered plan form. The distribution of the airfoil chord along the span is elliptical for the tail under consideration.

The hinge axis having been located, the effective parameters for the hinge-moment and the pitching-moment coefficients may be determined in the manner already outlined. For the problem under consideration, this process has been carried out in detail and the following values for the parameters have been obtained:

$$\left(\frac{\partial c_{h_f}}{\partial \delta_f} \right)_{c_n, \delta_t} = -0.0076$$

$$\left(\frac{\partial c_{h_f}}{\partial c_n} \right)_{\delta_f, \delta_t} = -0.093$$

$$\left(\frac{\partial c_{h_f}}{\partial \delta_t} \right)_{c_n, \delta_f} = -0.0032 \text{ (approx., by interpolation)}$$

$$\left(\frac{\partial \alpha}{\partial \delta_t} \right)_{c_n, \delta_f} = -0.06 \text{ (approx.)}$$

Stick Force

- (1) To compute the stick force, the hinge-moment parameters C_N' , δ_f' , and δ_t' being known, solve for C_{h_f}' by using equation (3).

For the example cited:

$$C_N' = -0.17$$

$$\delta_t' = 15^\circ$$

$$\delta_f' = -26^\circ$$

Therefore

$$\begin{aligned} C_{hf}' &= (-0.093)(-0.17) + (-0.0076)(-26) + (-0.0032)(15) \\ &= 0.165 \end{aligned}$$

(2) The stick force is

$$F_s = \frac{C_{hf}' (\bar{c}_f')^2 b' \bar{q}' \delta_f'}{s(\delta_s)} \quad (17)$$

For the example cited, $\bar{c}_f' = 1.48$ feet

When the airplane is landed at 70 miles per hour, the dynamic pressure at the tail is

$$\begin{aligned} \bar{q}' &= q \frac{\bar{q}'}{q} \\ &= \frac{0.002378}{2} (70 \times 1.47)^2 (0.96) \\ &= 12.1 \text{ pounds per square foot} \end{aligned}$$

$$\begin{aligned} \text{and } F_s &= \frac{(0.165)(1.48)^2 (12.8)(12.1)(-26)}{(1.75)(30)} \\ &= -27.7 \text{ pounds} \end{aligned}$$

In order to visualize more clearly the effect of flap chord on the stick force, calculations were made for a rectangular tail having flaps of various ratios of c_f'/c' for the conditions of tab neutral and deflected 15° . The results are plotted in figure 6. In each case the C_N' required was -0.17 and the maximum allowable flap deflection for the particular c_f'/c' value was used. It should also be pointed out that the stick length and the maximum stick deflection were held constant, which resulted in an increased mechanical advantage δ_f'/δ_s for large-chord flaps. The curves indicate that a given size tab is much more effective in reducing stick forces of large-chord flaps than small-chord flaps. This result is an expected one because figure 2(c) indicates the same result when hinge moments rather than hinge-moment coefficients are considered. The computations also show that the highest stick forces occur in the range of c_f'/c'

most commonly used in present-day practice: from 0.40 to 0.60.

Tab and Flap Deflections to Trim

It is considered desirable to install a trimming tab effective enough to trim the airplane when an approach for landing is being made. If, for this condition, the angle of attack for the tail and the normal-force coefficient required of the tail are known, the tab setting to trim with zero stick force may be computed from equation (5). For the airplane used in the example to glide in equilibrium at 110 miles per hour, it is computed that

$$\alpha_a' = -1.2^\circ$$

$$C_N' = -0.14$$

Calculate the slope of the lift curve in free air by equation (11).

$$\left(\frac{\partial C_N}{\partial \alpha} \right)_{\delta_f, \delta_t} = 0.852 \left(\frac{0.095}{1 + \frac{57.3 (0.095)}{\pi(3.4)}} \right) = 0.054$$

Therefore from equation (5)

$$\begin{aligned} \delta_t' (C_{H_f}=0) &= \frac{-0.14 \left[-\frac{1}{(0.054)(-0.67)} + \frac{(-0.093)}{(-0.0076)} \right] + \frac{(-1.2)}{(-0.67)}}{\left[\frac{(-0.06)}{(-0.67)} - \frac{(-0.0032)}{(-0.0076)} \right]} \\ &= 11.4^\circ \end{aligned}$$

The corresponding flap deflection required to maintain equilibrium may be computed from equation (6). Thus for the example cited

$$\delta_f' (C_{H_f}=0) = \frac{-1}{-0.67} \left[\frac{(-0.14)}{(0.054)} - (-1.2) + (-0.06)(11.4) \right] = -3.1^\circ$$

When the tab is used as a balancing tab, the free-floating angle of the flap may be computed from equation (7).

For the example cited:

$$\delta_t' = K\delta_f' + \delta_{t_0}', \text{ when } \delta_{t_0}' = 1^\circ \text{ and } K = -0.5$$

Thus, when $\alpha_a' = -1.2^\circ$,

$$\delta_f' (C_{hf}=0)$$

$$= \frac{(-0.093)(0.054)(-1.2) + [-(-0.093)(0.054)(-0.06) + (-0.0032)]}{-(-0.093)(0.054)(-0.67) + (-0.0076) + (-0.5)[-(-0.093)(0.054)(-0.06) + (-0.0032)]}$$

$$= 0.27^\circ$$

The corresponding normal-force coefficient of the tail is determined by equation (8). Thus for the example under consideration

$$C_N' (C_{hf}=0)$$

$$= 0.054 \{ (-1.2) - (-0.67)(0.27) - (-0.06) [1 + (-0.5)(0.27)] \}$$

$$= -0.05$$

The rate of change of free-floating angle with angle of attack may be calculated from equation (9).

Thus

$$\left(\frac{\partial \delta_f}{\partial \alpha} \right)_{C_{hf}=0}$$

$$= \frac{(-0.093)(0.054)}{-(-0.093)(0.054)(-0.67) + (-0.0076) + (-0.5)[-(-0.093)(0.054)(-0.06) + (-0.0032)]}$$

$$= -0.546$$

Similarly the slope of the lift curve for the tail with controls free is found from equation (10).

$$\left(\frac{\partial C_N}{\partial \alpha} \right)_{C_{hf}=0} = (0.054) \{ 1 - [(-0.67) + (-0.5)(-0.06)] (-0.546) \} = 0.035$$

APPLICATION OF DATA TO VERTICAL TAILS AND AILERONS

This entire procedure may be used equally well to calculate rudder size, with the obvious modification of substituting yawing-moment coefficients for pitching-moment coefficients and sidewash for downwash in calculating the normal-force coefficient required.

The section parameters presented in this report may also be used to compute aileron characteristics by means of the method outlined in reference 14.

Langley Memorial Aeronautical Laboratory,
National Advisory Committee for Aeronautics,
Langley Field, Va., December 30, 1940.

APPENDIX A

EQUATIONS OF THE THIN-AIRFOIL THEORY

Identification of Parameters

The conversion of the equations for the aerodynamic characteristics of a finite airfoil based on the thin-airfoil theory (reference 1, 2, and 3) from the old British system of aerodynamic coefficients to the standard NACA form and the use of symbols for the parameters, or slopes, in these equations has led to some misunderstanding as to the identity of these parameters. The purpose of this analysis is to clarify the identity of the parameters and to distinguish between the ones that are sometimes confused because of a similarity in form. In addition, a summary of the relations is given whereby other useful parameters not presented in figures 1 and 2 may be computed from these data.

If

$$C_N = f_1(\alpha, \delta_f, \delta_t)$$

it follows that

$$dC_N = \frac{\partial f_1}{\partial \alpha} d\alpha + \frac{\partial f_1}{\partial \delta_f} d\delta_f + \frac{\partial f_1}{\partial \delta_t} d\delta_t$$

which is identical to:

$$\begin{aligned} dC_N &= \frac{\partial C_N}{\partial \alpha} d\alpha + \frac{\partial C_N}{\partial \delta_f} d\delta_f + \frac{\partial C_N}{\partial \delta_t} d\delta_t \\ &= \frac{\partial C_N}{\partial \alpha} \left(d\alpha + \frac{\frac{\partial C_N}{\partial \delta_f}}{\frac{\partial C_N}{\partial \alpha}} d\delta_f + \frac{\frac{\partial C_N}{\partial \delta_t}}{\frac{\partial C_N}{\partial \alpha}} d\delta_t \right) \\ &= \frac{\partial C_N}{\partial \alpha} \left(d\alpha - \frac{\partial \alpha}{\partial \delta_f} d\delta_f - \frac{\partial \alpha}{\partial \delta_t} d\delta_t \right) \end{aligned}$$

Likewise if

$$C_m = f_2(C_N, \delta_f, \delta_t)$$

it follows that

$$dC_m = \frac{\partial C_m}{\partial C_N} dC_N + \frac{\partial C_m}{\partial \delta_f} d\delta_f + \frac{\partial C_m}{\partial \delta_t} d\delta_t$$

and if

$$C_{hf} = f_3(C_N, \delta_f, \delta_t)$$

Then

$$dC_{hf} = \frac{\partial C_{hf}}{\partial C_N} dC_N + \frac{\partial C_{hf}}{\partial \delta_f} d\delta_f + \frac{\partial C_{hf}}{\partial \delta_t} d\delta_t$$

or, if it is considered that

$$C_{hf} = f_4(\alpha, \delta_f, \delta_t)$$

$$dC_{hf} = \frac{\partial C_{hf}}{\partial \alpha} d\alpha + \frac{\partial C_{hf}}{\partial \delta_f} d\delta_f + \frac{\partial C_{hf}}{\partial \delta_t} d\delta_t$$

Because, according to the thin-airfoil theory, a linear relationship exists among the variables C_N , C_{hf} , C_m , α , δ_f , and δ_t , the total differential in the foregoing equations may be replaced by the variable. Because no change in circulation is involved, $\left(\frac{\partial \alpha}{\partial \delta_f}\right)_{C_N, \delta_t}$ is identical with $\left(\frac{\partial \alpha}{\partial \delta_f}\right)_{C_N, \delta_t}$, etc. The subscripts indicate the variables held constant when the partial differential is taken. The equations now become

$$C_N = \left(\frac{\partial C_N}{\partial \alpha}\right)_{\delta_f, \delta_t} \left[\alpha - \left(\frac{\partial \alpha}{\partial \delta_f}\right)_{C_N, \delta_t} \delta_f - \left(\frac{\partial \alpha}{\partial \delta_t}\right)_{C_N, \delta_f} \delta_t \right] \quad (1)$$

$$C_m = \left(\frac{\partial C_m}{\partial C_N}\right)_{\delta_f, \delta_t} C_N + \left(\frac{\partial C_m}{\partial \delta_f}\right)_{C_N, \delta_t} \delta_f + \left(\frac{\partial C_m}{\partial \delta_t}\right)_{C_N, \delta_f} \delta_t \quad (2)$$

$$C_{hf} = \left(\frac{\partial C_{hf}}{\partial c_n} \right)_{\delta_f, \delta_t} c_N + \left(\frac{\partial C_{hf}}{\partial \delta_f} \right)_{c_n, \delta_t} \delta_f + \left(\frac{\partial C_{hf}}{\partial \delta_t} \right)_{c_n, \delta_f} \delta_t \quad (3)$$

$$C_{hf} = \left(\frac{\partial C_{hf}}{\partial \alpha} \right)_{\delta_f, \delta_t} \alpha + \left(\frac{\partial C_{hf}}{\partial \delta_f} \right)_{\alpha, \delta_t} \delta_f + \left(\frac{\partial C_{hf}}{\partial \delta_t} \right)_{\alpha, \delta_f} \delta_t \quad (4)$$

These equations are of the same form as those presented in references 2, 3, and 5. By comparison it is possible to define the various constants of the equations in these references in terms of the variables involved. In order to indicate from which relationships the various partial derivatives are determined, subscripts are added to the derivatives to indicate the variables held constant in taking the partial derivative.

The following table of corresponding symbols has been prepared for future reference. The parameters from references 2 and 3 are, for obvious reasons, expressed in terms of the old British system of coefficients; the angles were measured in radians; the pitching moment was measured about the airfoil nose.

Parameter	NACA system of coefficients	Old British system of coefficients	
	Reference 5	Reference 2	Reference 3
$\left(\frac{\partial C_N}{\partial \alpha} \right)_{\delta_f, \delta_t}$	a_1	a_1	a_1
$\left(\frac{\partial C_N}{\partial \delta_f} \right)_{\alpha, \delta_t}$	---	a_2	---
$\left(\frac{\partial \alpha}{\partial \delta_f} \right)_{c_n, \delta_t}$	$-\lambda_1$	$-\frac{a_2}{a_1}$	$-\lambda_5$ or $-\lambda_1$
$\left(\frac{\partial \alpha}{\partial \delta_t} \right)_{c_n, \delta_f}$	$-\lambda_2$	---	$-\lambda_5$ or $-\lambda_2$

Parameter	NACA system of coefficients	Old British system of coefficients	
	Reference 5	Reference 2	Reference 3
$\left(\frac{\partial c_m}{\partial c_n}\right)_{\delta_f, \delta_t}$	----	$-\frac{1}{4}$	$-\frac{1}{4}$
$\left(\frac{\partial c_m}{\partial \delta_f}\right)_{c_n, \delta_t}$	----	$-m$	$-m_s$ or $-m_1$
$\left(\frac{\partial c_m}{\partial \delta_t}\right)_{c_n, \delta_f}$	----	----	$-m_s$ or $-m_2$
$\left(\frac{\partial c_{hf}}{\partial \alpha}\right)_{\delta_f, \delta_t}$	----	$-b_1$	----
$\left(\frac{\partial c_{hf}}{\partial \delta_f}\right)_{\alpha, \delta_t}$	----	$-b_2$	----
$\left(\frac{\partial c_{hf}}{\partial c_n}\right)_{\delta_f, \delta_t}$	$-u$	$-\frac{b_1}{a_1}$	$-\beta_r$
$\left(\frac{\partial c_{hf}}{\partial \delta_f}\right)_{c_n, \delta_t}$	$-v_{11}$	$-b = \frac{b_2 a_1 - b_1 a_2}{a_1}$	$-b_{rr}$ or $-b_{1,1}$
$\left(\frac{\partial c_{hf}}{\partial \delta_t}\right)_{c_n, \delta_f}$	v_{12}	----	$-b_{rs}$ or $-b_{1,2}$

Summary of Relationships

The slopes summarized in the following equations are useful for design purposes and may be computed with the aid of the charts of figures 1 and 2.

$$\left(\frac{\partial c_N}{\partial \delta_f}\right)_{\alpha, \delta_t} = - \left(\frac{\partial c_N}{\partial \alpha}\right)_{\delta_f, \delta_t} \left(\frac{\partial \alpha}{\partial \delta_f}\right)_{c_n, \delta_t}$$

$$\left(\frac{\partial c_N}{\partial \delta_t}\right)_{\alpha, \delta_f} = - \left(\frac{\partial c_N}{\partial \alpha}\right)_{\delta_f, \delta_t} \left(\frac{\partial \alpha}{\partial \delta_t}\right)_{c_n, \delta_f}$$

$$\left(\frac{\partial c_n}{\partial \delta_f}\right)_{c_{hf}, \delta_t} = - \frac{\left(\frac{\partial c_{hf}}{\partial \delta_f}\right)_{c_n, \delta_t}}{\left(\frac{\partial c_{hf}}{\partial c_n}\right)_{\delta_f, \delta_t}}$$

$$\left(\frac{\partial c_{hf}}{\partial \alpha}\right)_{\delta_f, \delta_t} = \left(\frac{\partial c_{hf}}{\partial c_n}\right)_{\delta_f, \delta_t} \left(\frac{\partial c_N}{\partial \alpha}\right)_{\delta_f, \delta_t}$$

$$\left(\frac{\partial c_{hf}}{\partial \delta_f}\right)_{\alpha, \delta_t} = - \left(\frac{\partial c_{hf}}{\partial \alpha}\right)_{\delta_f, \delta_t} \left(\frac{\partial \alpha}{\partial \delta_f}\right)_{c_n, \delta_t} + \left(\frac{\partial c_{hf}}{\partial \delta_f}\right)_{c_n, \delta_t}$$

$$\left(\frac{\partial c_{hf}}{\partial \delta_t}\right)_{\alpha, \delta_f} = - \left(\frac{\partial c_{hf}}{\partial \alpha}\right)_{\delta_f, \delta_t} \left(\frac{\partial \alpha}{\partial \delta_t}\right)_{c_n, \delta_f} + \left(\frac{\partial c_{hf}}{\partial \delta_t}\right)_{c_n, \delta_f}$$

$$\left(\frac{\partial c_m}{\partial c_N}\right)_{\delta_f, \delta_t} = \frac{\left(\frac{\partial c_m}{\partial \alpha}\right)_{\delta_f, \delta_t}}{\left(\frac{\partial c_N}{\partial \alpha}\right)_{\delta_f, \delta_t}}$$

$$\left(\frac{\partial c_m}{\partial \delta_f}\right)_{\alpha, \delta_t} = - \left(\frac{\partial c_m}{\partial \alpha}\right)_{\delta_f, \delta_t} \left(\frac{\partial \alpha}{\partial \delta_f}\right)_{c_n, \delta_t} + \left(\frac{\partial c_m}{\partial \delta_f}\right)_{c_n, \delta_t}$$

$$\left(\frac{\partial c_m}{\partial \delta_t}\right)_{\alpha, \delta_f} = - \left(\frac{\partial c_m}{\partial \alpha}\right)_{\delta_f, \delta_t} \left(\frac{\partial \alpha}{\partial \delta_t}\right)_{c_n, \delta_f} + \left(\frac{\partial c_m}{\partial \delta_t}\right)_{c_n, \delta_f}$$

$$\left(\frac{\partial \delta_f}{\partial \delta_t}\right)_{c_n, \alpha} = - \frac{\left(\frac{\partial c_N}{\partial \delta_t}\right)_{\alpha, \delta_f}}{\left(\frac{\partial c_N}{\partial \delta_f}\right)_{\alpha, \delta_t}} = - \frac{\left(\frac{\partial \alpha}{\partial \delta_t}\right)_{c_n, \delta_f}}{\left(\frac{\partial \alpha}{\partial \delta_f}\right)_{c_n, \delta_t}}$$

$$\left(\frac{\partial \delta_f}{\partial \delta_t}\right)_{c_{hf}, \alpha} = - \frac{\left(\frac{\partial c_{hf}}{\partial \delta_t}\right)_{\alpha, \delta_f}}{\left(\frac{\partial c_{hf}}{\partial \delta_f}\right)_{\alpha, \delta_t}}$$

APPENDIX B

DEVELOPMENT OF FORMULAS FOR TRIM, BALANCE,
AND FREE-CONTROL CONDITIONS

For an airfoil with a flap and a trimming tab, the formula for the tab deflection required to trim, where for trim C_{hf} is 0, was developed in the following manner.

From the thin-airfoil theory (see appendix A)

$$C_N = \left(\frac{\partial C_N}{\partial \alpha} \right)_{\delta_f, \delta_t} \left[\alpha_a - \left(\frac{\partial \alpha}{\partial \delta_f} \right)_{c_n, \delta_t} \delta_f - \left(\frac{\partial \alpha}{\partial \delta_t} \right)_{c_n, \delta_f} \delta_t \right] \quad (1)$$

$$C_{hf} = \left(\frac{\partial C_{hf}}{\partial c_n} \right)_{\delta_f, \delta_t} C_N + \left(\frac{\partial C_{hf}}{\partial \delta_f} \right)_{c_n, \delta_t} \delta_f + \left(\frac{\partial C_{hf}}{\partial \delta_t} \right)_{c_n, \delta_f} \delta_t \quad (3)$$

Solve for δ_f in equation (1):

$$\delta_f = - \frac{\left[C_N - \left(\frac{\partial C_N}{\partial \alpha} \right)_{\delta_f, \delta_t} \alpha_a + \left(\frac{\partial C_N}{\partial \alpha} \right)_{\delta_f, \delta_t} \left(\frac{\partial \alpha}{\partial \delta_t} \right)_{c_n, \delta_f} \delta_t \right]}{\left(\frac{\partial C_N}{\partial \alpha} \right)_{\delta_f, \delta_t} \left(\frac{\partial \alpha}{\partial \delta_f} \right)_{c_n, \delta_t}} \quad (1a)$$

Because $C_{hf} = 0$ to trim, equation (3) may be equated to 0. Solve for $\delta_f (C_{hf} = 0)$ and obtain

$$\delta_f (C_{hf} = 0) = - \frac{\left[\left(\frac{\partial C_{hf}}{\partial c_n} \right)_{\delta_f, \delta_t} C_N + \left(\frac{\partial C_{hf}}{\partial \delta_t} \right)_{c_n, \delta_f} \delta_t \right]}{\left(\frac{\partial C_{hf}}{\partial \delta_f} \right)_{c_n, \delta_t}} \quad (3a)$$

If C_N for $C_{hf} = 0$ is substituted for C_N in equation

(1a), δ_f will become $\delta_f(C_{h_f}=0)$. Now equations (1a) and (3a) may be equated and the resultant expression may be solved for δ_t to trim $\delta_t(C_{h_f}=0)$.

$$\delta_t(C_{h_f}=0) = \frac{C_N(C_{h_f}=0) \left[-\frac{1}{\left(\frac{\partial C_N}{\partial \alpha}\right)_{\delta_f, \delta_t} \left(\frac{\partial \alpha}{\partial \delta_f}\right)_{c_n, \delta_t} + \left(\frac{\partial C_{h_f}}{\partial \delta_f}\right)_{c_n, \delta_t}} + \frac{\alpha_a}{\left(\frac{\partial \alpha}{\partial \delta_f}\right)_{c_n, \delta_t}} \right]}{\frac{\left(\frac{\partial \alpha}{\partial \delta_t}\right)_{c_n, \delta_f}}{\left(\frac{\partial \alpha}{\partial \delta_f}\right)_{c_n, \delta_t}} - \frac{\left(\frac{\partial C_{h_f}}{\partial \delta_t}\right)_{c_n, \delta_f}}{\left(\frac{\partial C_{h_f}}{\partial \delta_f}\right)_{c_n, \delta_t}}}$$

(5)

In this form the tab deflection to trim may be determined by direct substitution of the values for the parameters as given in the data for this report.

The flap deflection with the tab set to trim may be determined from equation (1a), which, when combined and rewritten, becomes

$$\delta_f(C_{h_f}=0) = -\frac{1}{\left(\frac{\partial \alpha}{\partial \delta_f}\right)_{c_n, \delta_t}} \left[\frac{C_N(C_{h_f}=0)}{\left(\frac{\partial C_N}{\partial \alpha}\right)_{\delta_f, \delta_t}} - \alpha_a + \left(\frac{\partial \alpha}{\partial \delta_t}\right)_{c_n, \delta_f} \delta_t(C_{h_f}=0) \right] \quad (6)$$

The equations for an airfoil and a flap with a balancing tab were derived as follows:

For a balancing tab, δ_t is $f(\delta_f)$, so that $\delta_t = K\delta_f + \delta_{t_0}$, where K is a constant for a linear variation of δ_t with δ_f , and δ_{t_0} is the initial tab setting. Therefore equations (1) and (3) become

$$C_N = \left(\frac{\partial C_N}{\partial \alpha}\right)_{\delta_f, \delta_t} \left[\alpha_a - \left(\frac{\partial \alpha}{\partial \delta_f}\right)_{c_n, \delta_t} \delta_f - \left(\frac{\partial \alpha}{\partial \delta_t}\right)_{c_n, \delta_f} (K\delta_f + \delta_{t_0}) \right]$$

and

$$C_{h_f} = \left(\frac{\partial C_{h_f}}{\partial C_N} \right)_{\delta_f, \delta_t} C_N + \left(\frac{\partial C_{h_f}}{\partial \delta_f} \right)_{C_N, \delta_t} \delta_f + \left(\frac{\partial C_{h_f}}{\partial \delta_t} \right)_{C_N, \delta_f} (K\delta_f + \delta_{t_0})$$

With controls free, $C_{h_f} = 0$, and equation (3) becomes

$$0 = \left(\frac{\partial C_{h_f}}{\partial C_N} \right)_{\delta_f, \delta_t} C_N + \left(\frac{\partial C_{h_f}}{\partial \delta_f} \right)_{C_N, \delta_t} \delta_f (C_{h_f}=0) + \left(\frac{\partial C_{h_f}}{\partial \delta_t} \right)_{C_N, \delta_f} (K\delta_f (C_{h_f}=0) + \delta_{t_0})$$

Revise equation (1) by changing C_N to $C_N(C_{h_f}=0)$

and substitute $\delta_f(C_{h_f}=0)$ for δ_f ; use this ex-

pression for $C_N(C_{h_f}=0)$ in the foregoing relation,

and the flap angle for control-free condition be-
comes

$$\delta_f(C_{hf}=0)$$

$$= - \left\{ \frac{\left(\frac{\partial C_{hf}}{\partial c_n} \right)_{\delta_f, \delta_t} \left(\frac{\partial C_N}{\partial \alpha} \right)_{\delta_f, \delta_t} \alpha_a + \left[- \left(\frac{\partial C_{hf}}{\partial c_n} \right)_{\delta_f, \delta_t} \left(\frac{\partial C_N}{\partial \alpha} \right)_{\delta_f, \delta_t} \left(\frac{\partial \alpha}{\partial \delta_t} \right)_{c_n, \delta_f} + \left(\frac{\partial C_{hf}}{\partial \delta_t} \right)_{c_n, \delta_f} \right] \delta_{t_0}}{- \left(\frac{\partial C_{hf}}{\partial c_n} \right)_{\delta_f, \delta_t} \left(\frac{\partial C_N}{\partial \alpha} \right)_{\delta_f, \delta_t} \left(\frac{\partial \alpha}{\partial \delta_f} \right)_{c_n, \delta_t} + \left(\frac{\partial C_{hf}}{\partial \delta_f} \right)_{c_n, \delta_t} + \left[- \left(\frac{\partial C_{hf}}{\partial c_n} \right)_{\delta_f, \delta_t} \left(\frac{\partial C_N}{\partial \alpha} \right)_{\delta_f, \delta_t} \left(\frac{\partial \alpha}{\partial \delta_t} \right)_{c_n, \delta_f} + \left(\frac{\partial C_{hf}}{\partial \delta_t} \right)_{c_n, \delta_f} \right]} \right\} \quad (7)$$

The equation for the normal-force coefficient with free controls is obtained by substituting the free-floating flap deflection from equation (7) into equation (1).

Thus

$$C_{N(C_{hf}=0)} = \left(\frac{\partial C_N}{\partial \alpha} \right)_{\delta_f, \delta_t} \left[\alpha_a - \left(\frac{\partial \alpha}{\partial \delta_f} \right)_{c_n, \delta_t} \delta_f(C_{hf}=0) - \left(\frac{\partial \alpha}{\partial \delta_t} \right)_{c_n, \delta_f} \left(K \delta_f(C_{hf}=0) + \delta_{t_0} \right) \right] \quad (8)$$

By the actual substitution of the right-hand member of equation (7), this equation may be written as

$$C_N(C_{hf}=0) = \left(\frac{\partial C_N}{\partial \alpha} \right)_{\delta_f, \delta_t} \left\{ \alpha_a - \left(\frac{\partial \alpha}{\partial \delta_t} \right)_{c_n, \delta_f} \delta_{t_0} + \left[\left(\frac{\partial \alpha}{\partial \delta_f} \right)_{c_n, \delta_t} + K \left(\frac{\partial \alpha}{\partial \delta_t} \right)_{c_n, \delta_f} \right] \right.$$

$$\left. \begin{aligned} & \left(\frac{\partial C_{hf}}{\partial c_n} \right)_{\delta_f, \delta_t} \left(\frac{\partial C_N}{\partial \alpha} \right)_{\delta_f, \delta_t} \alpha_a + \left[- \left(\frac{\partial C_{hf}}{\partial c_n} \right)_{\delta_f, \delta_t} \left(\frac{\partial C_N}{\partial \alpha} \right)_{\delta_f, \delta_t} \left(\frac{\partial \alpha}{\partial \delta_t} \right)_{c_n, \delta_f} + \left(\frac{\partial C_{hf}}{\partial \delta_t} \right)_{c_n, \delta_f} \right] \delta_{t_0} \\ & - \left(\frac{\partial C_{hf}}{\partial c_n} \right)_{\delta_f, \delta_t} \left(\frac{\partial C_N}{\partial \alpha} \right)_{\delta_f, \delta_t} \left(\frac{\partial \alpha}{\partial \delta_f} \right)_{c_n, \delta_t} + \left(\frac{\partial C_{hf}}{\partial \delta_f} \right)_{c_n, \delta_t} + K \left[- \left(\frac{\partial C_{hf}}{\partial c_n} \right)_{\delta_f, \delta_t} \left(\frac{\partial C_N}{\partial \alpha} \right)_{\delta_f, \delta_t} \left(\frac{\partial \alpha}{\partial \delta_t} \right)_{c_n, \delta_f} + \left(\frac{\partial C_{hf}}{\partial \delta_t} \right)_{c_n, \delta_f} \right] \end{aligned} \right\}$$

(8a)

By the differentiation of equation (7) with respect to α , δ_{t_0} being a constant, the stabilizing factor becomes

$$\begin{aligned} & \left(\frac{\partial \delta_f}{\partial \alpha} \right)_{C_{hf}=0} \\ & = \frac{\left(\frac{\partial C_{hf}}{\partial c_n} \right)_{\delta_f, \delta_t} \left(\frac{\partial C_N}{\partial \alpha} \right)_{\delta_f, \delta_t}}{- \left(\frac{\partial C_{hf}}{\partial c_n} \right)_{\delta_f, \delta_t} \left(\frac{\partial C_N}{\partial \alpha} \right)_{\delta_f, \delta_t} \left(\frac{\partial \alpha}{\partial \delta_f} \right)_{c_n, \delta_t} + \left(\frac{\partial C_{hf}}{\partial \delta_f} \right)_{c_n, \delta_t} + K \left[- \left(\frac{\partial C_{hf}}{\partial c_n} \right)_{\delta_f, \delta_t} \left(\frac{\partial C_N}{\partial \alpha} \right)_{\delta_f, \delta_t} \left(\frac{\partial \alpha}{\partial \delta_t} \right)_{c_n, \delta_f} + \left(\frac{\partial C_{hf}}{\partial \delta_t} \right)_{c_n, \delta_f} \right]} \end{aligned}$$

(9)

If equation (8) is differentiated with respect to α , the slope of the normal-force coefficient curve becomes

$$\left(\frac{\partial C_N}{\partial \alpha}\right)_{C_{hf}=0} = \left(\frac{\partial C_N}{\partial \alpha}\right)_{\delta_f, \delta_t} \left\{ 1 - \left[\left(\frac{\partial \alpha}{\partial \delta_f}\right)_{c_n, \delta_t} + K \left(\frac{\partial \alpha}{\partial \delta_t}\right)_{c_n, \delta_f} \right] \left(\frac{\partial \delta_f}{\partial \alpha}\right)_{C_{hf}=0} \right\} \quad (10)$$

or by differentiation of equation (8a)

$$\left(\frac{\partial C_N}{\partial \alpha}\right)_{C_{hf}=0} = \left(\frac{\partial C_N}{\partial \alpha}\right)_{\delta_f, \delta_t} \left\{ 1 + \left[\left(\frac{\partial \alpha}{\partial \delta_f}\right)_{c_n, \delta_t} + K \left(\frac{\partial \alpha}{\partial \delta_t}\right)_{c_n, \delta_f} \right] \frac{\left(\frac{\partial C_{hf}}{\partial c_n}\right)_{\delta_f, \delta_t} \left(\frac{\partial C_N}{\partial \alpha}\right)_{\delta_f, \delta_t}}{\left[-\left(\frac{\partial C_{hf}}{\partial c_n}\right)_{\delta_f, \delta_t} \left(\frac{\partial C_N}{\partial \alpha}\right)_{\delta_f, \delta_t} \left(\frac{\partial \alpha}{\partial \delta_f}\right)_{c_n, \delta_t} + \left(\frac{\partial C_{hf}}{\partial \delta_f}\right)_{c_n, \delta_t} + K \left[-\left(\frac{\partial C_{hf}}{\partial c_n}\right)_{\delta_f, \delta_t} \left(\frac{\partial C_N}{\partial \alpha}\right)_{\delta_f, \delta_t} \left(\frac{\partial \alpha}{\partial \delta_t}\right)_{c_n, \delta_f} + \left(\frac{\partial C_{hf}}{\partial \delta_t}\right)_{c_n, \delta_f} \right] } \right\} \quad (10a)$$

By the use of the slope relations summarized at the end of appendix A, it can easily be shown that equations (5), (6), (7), and (9) may be considerably simplified. When this simplification has been made, these equations read as follows:

$$\delta_t(C_{hf}=0) = \frac{\frac{C_N(C_{hf}=0)}{\left(\frac{\partial C_N}{\partial \delta_f}\right)_{\alpha, \delta_t}} - \frac{C_N(C_{hf}=0)}{\left(\frac{\partial c_n}{\partial \delta_f}\right)_{C_{hf}, \delta_t}} + \frac{\alpha_a}{\left(\frac{\partial \alpha}{\partial \delta_f}\right)_{c_n, \delta_t}}}{-\left(\frac{\partial \delta_f}{\partial \delta_t}\right)_{c_n, \alpha} + \left(\frac{\partial \delta_f}{\partial \delta_t}\right)_{C_{hf}, \alpha}} \quad (5a)$$

$$\delta_f(C_{hf}=0) = \frac{\frac{C_N(C_{hf}=0)}{\left(\frac{\partial C_N}{\partial \delta_f}\right)_{\alpha, \delta_t}} + \frac{\alpha_a}{\left(\frac{\partial \alpha}{\partial \delta_f}\right)_{c_n, \delta_t}} + \frac{\delta_t(C_{hf}=0)}{\left(\frac{\partial \delta_t}{\partial \delta_f}\right)_{c_n, \alpha}}}{\left(\frac{\partial \delta_f}{\partial \delta_t}\right)_{c_n, \alpha}} \quad (6a)$$

$$\delta_f(C_{hf}=0) = - \frac{\left(\frac{\partial c_{hf}}{\partial \alpha}\right)_{\delta_f, \delta_t} \alpha_a + \left(\frac{\partial c_{hf}}{\partial \delta_t}\right)_{\alpha, \delta_f} \delta_{t0}}{\left(\frac{\partial c_{hf}}{\partial \delta_f}\right)_{\alpha, \delta_t} + K \left(\frac{\partial c_{hf}}{\partial \delta_t}\right)_{\alpha, \delta_f}} \quad (7a)$$

$$\left(\frac{\partial \delta_f}{\partial \alpha}\right)_{C_{hf}=0} = - \frac{\left(\frac{\partial c_{hf}}{\partial \alpha}\right)_{\delta_f, \delta_t}}{\left(\frac{\partial c_{hf}}{\partial \delta_f}\right)_{\alpha, \delta_t} + K \left(\frac{\partial c_{hf}}{\partial \delta_t}\right)_{\alpha, \delta_f}} \quad (9a)$$

$$\left(\frac{\partial C_N}{\partial \alpha}\right)_{C_{hf}=0} = \left(\frac{\partial C_N}{\partial \alpha}\right)_{\delta_f, \delta_t} \left[\frac{\left(\frac{\partial c_{hf}}{\partial \delta_f}\right)_{c_n, \delta_t} + K \left(\frac{\partial c_{hf}}{\partial \delta_t}\right)_{c_n, \delta_f}}{\left(\frac{\partial c_{hf}}{\partial \delta_f}\right)_{\alpha, \delta_t} + K \left(\frac{\partial c_{hf}}{\partial \delta_t}\right)_{\alpha, \delta_f}} \right] \quad (10b)$$

REFERENCES

1. Glauert, H.: A Theory of Thin Aerofoils. R. & M. No. 910, British A.R.C., 1924.
2. Glauert, H.: Theoretical Relationships for an Aerofoil with Hinged Flap. R. & M. No. 1095, British A.R.C., 1927.
3. Perring, W. G. A.: The Theoretical Relationships for an Aerofoil with a Multiply Hinged Flap System. R. & M. No. 1171, British A.R.C., 1928.
4. Silverstein, Abe, and Katzoff, S.: Aerodynamic Characteristics of Horizontal Tail Surfaces. Rep. No. 688, NACA, 1940.
5. Goett, Harry J., and Reeder, J. P.: Effects of Elevator Nose Shape, Gap, Balance, and Tabs on the Aerodynamic Characteristics of a Horizontal Tail Surface. Rep. No. 675, NACA, 1939.
6. Silverstein, Abe: Toward a Rational Method of Tailplane Design. Jour. Aero. Sci., vol. 6, no. 9, July 1939, pp. 361-69.
7. Street, William G., and Ames, Milton B., Jr.: Pressure-Distribution Investigation of an N.A.C.A. 0009 Airfoil with a 50-Percent-Chord Plain Flap and Three Tabs. T.N. No. 734, NACA, 1939.
8. Ames, Milton B., Jr., and Sears, Richard I.: Pressure-Distribution Investigation of an N.A.C.A. 0009 Airfoil with a 30-Percent-Chord Plain Flap and Three Tabs. T.N. No. 759, NACA, 1940.
9. Ames, Milton B., Jr., and Sears, Richard I.: Pressure-Distribution Investigation of an N.A.C.A. 0009 Airfoil with an 80-Percent-Chord Plain Flap and Three Tabs. T.N. No. 761, NACA, 1940.
10. Harris, Thomas A.: Reduction of Hinge Moments of Airplane Control Surfaces by Tabs. Rep. No. 528, NACA, 1935.
11. Anderson, Raymond F.: Determination of the Characteristics of Tapered Wings. Rep. No. 572, NACA, 1936.

12. Silverstein, Abe, and Katzoff, S.: Design Charts for Predicting Downwash Angles and Wake Characteristics behind Plain and Flapped Wings. Rep. No. 648, NACA, 1939.
13. Prandtl, L.: Induced Drag of Multiplanes. T.N. No. 182, NACA, 1924.
14. Weick, Fred E., and Jones, Robert T.: Résumé and Analysis of N.A.C.A. Lateral Control Research. Rep. No. 605, NACA, 1937.

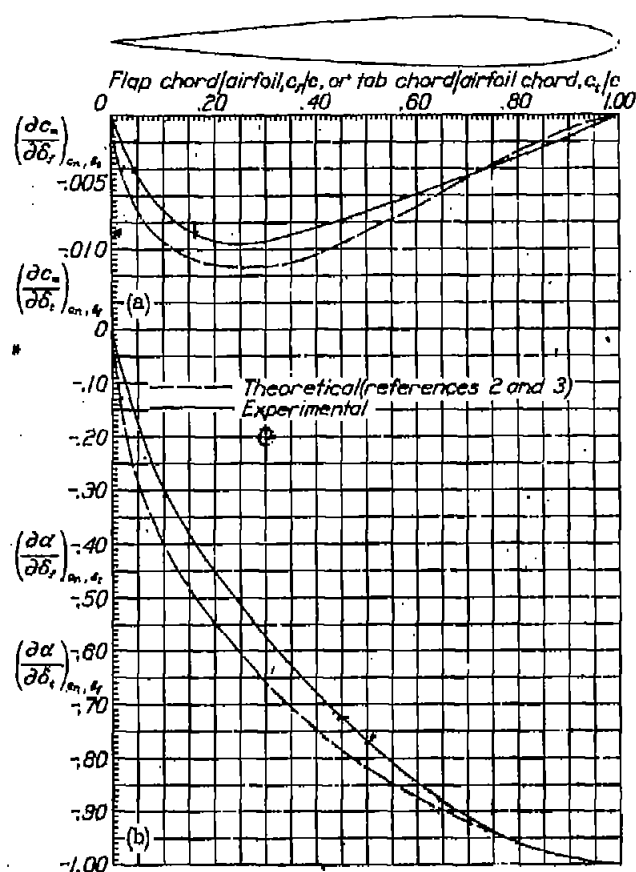
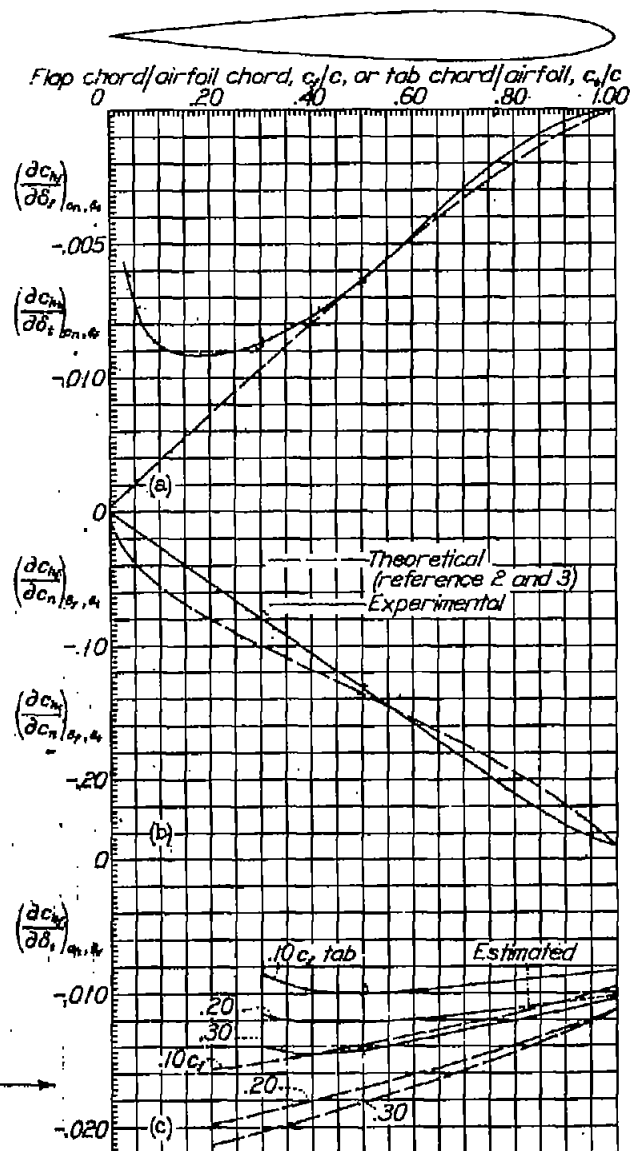


Figure 1.- Variation of $(\frac{\partial c_m}{\partial \delta})_{\alpha, \delta_f}$ and $(\frac{\partial \alpha}{\partial \delta})_{\alpha, \delta_f}$ with c_f/c or c_t/c for the NACA 0009 airfoil.
(a) $(\frac{\partial c_m}{\partial \delta})_{\alpha, \delta_f}$; (b) $(\frac{\partial \alpha}{\partial \delta})_{\alpha, \delta_f}$

Figure 2.- Variation of $(\frac{\partial c_m}{\partial \delta})_{\alpha, \delta_f}$, $(\frac{\partial c_m}{\partial c_n})_{\delta_f, \delta_t}$, and $(\frac{\partial c_m}{\partial \delta_t})_{\alpha, \delta_f}$ with c_f/c or c_t/c for the NACA 0009 airfoil. (a) $(\frac{\partial c_m}{\partial \delta})_{\alpha, \delta_f}$; (b) $(\frac{\partial c_m}{\partial c_n})_{\delta_f, \delta_t}$; (c) $(\frac{\partial c_m}{\partial \delta_t})_{\alpha, \delta_f}$.



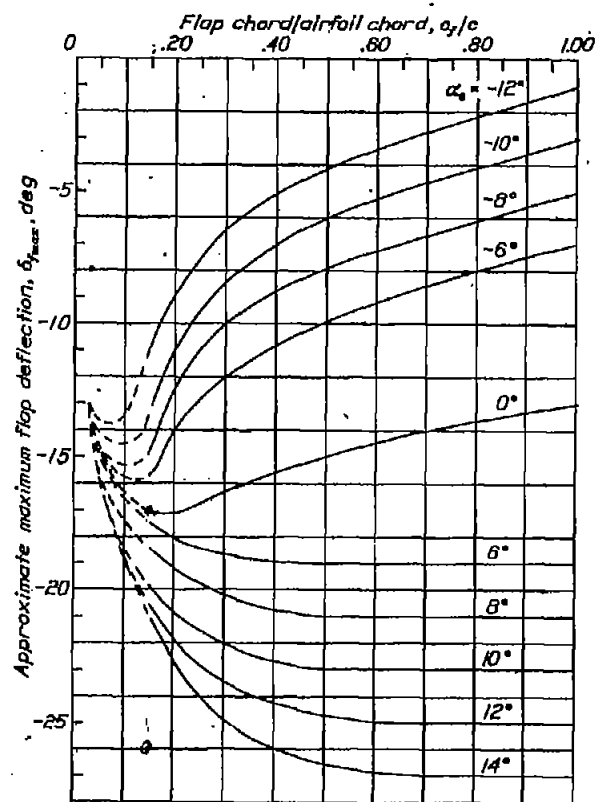
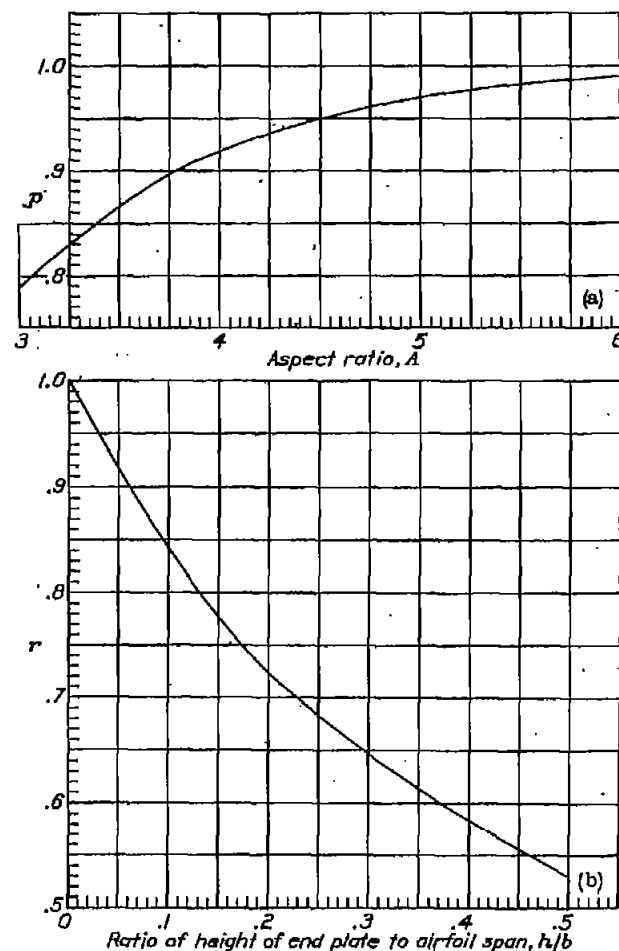


Figure 3.- Approximate maximum allowable flap deflections for linear limits of airfoil characteristics at various angles of attack. Data for NACA 0009 airfoil with infinite aspect ratio and at an effective Reynolds number of 3,410,000.



(a) Variation of parameter p with A for airfoils without end plates.
(b) Variation of parameter r with h/b. For horizontal surfaces with end plates, $p = 1$. For horizontal surfaces with single vertical surfaces, $r = 1$. Values of r taken from reference 4.

Figure 4.- Parameters p and r for correction of parameter, $\left(\frac{\partial C_N}{\partial \alpha}\right)_\delta$.

$$\left(\frac{\partial C_N}{\partial \alpha}\right)_{\delta_f, \delta_t} = p \frac{\left(\frac{\partial C_N}{\partial \alpha}\right)_{\delta_f, \delta_t}}{1 + [57.3 r \left(\frac{\partial C_N}{\partial \alpha}\right)_{\delta_f, \delta_t} / \pi A]}$$

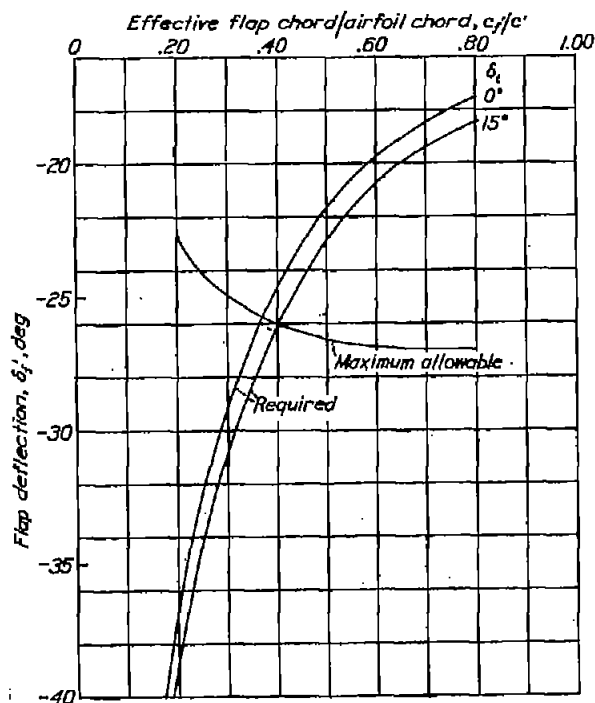


Figure 5.- Required flap deflections for tab neutral and deflected 15° and maximum allowable flap deflections for various values of c_f'/c . A_0' , 4.2; α_{θ}' , 14.0°; c_t'/c , 0.06.

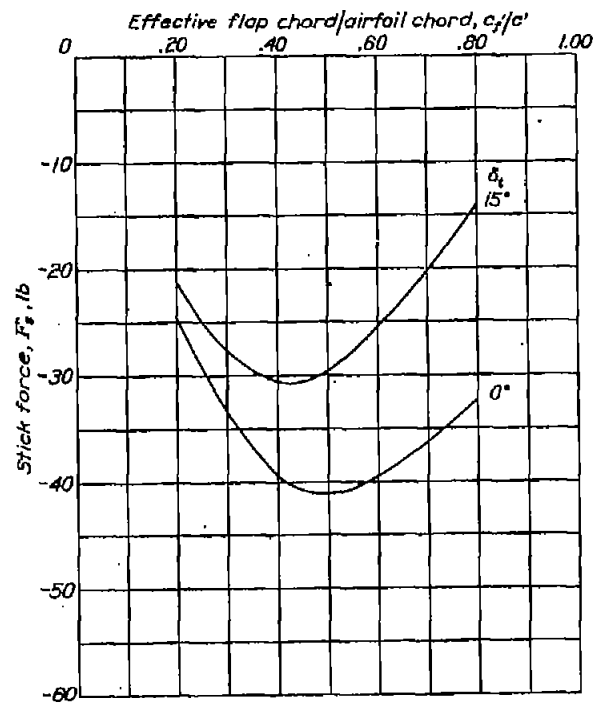


Figure 6.- Required stick force for tab neutral and deflected 15° for landing with rectangular tails for various values of c_f'/c . A_0' , 4.2; α_{θ}' , 14.0°; c_t'/c , 0.06.

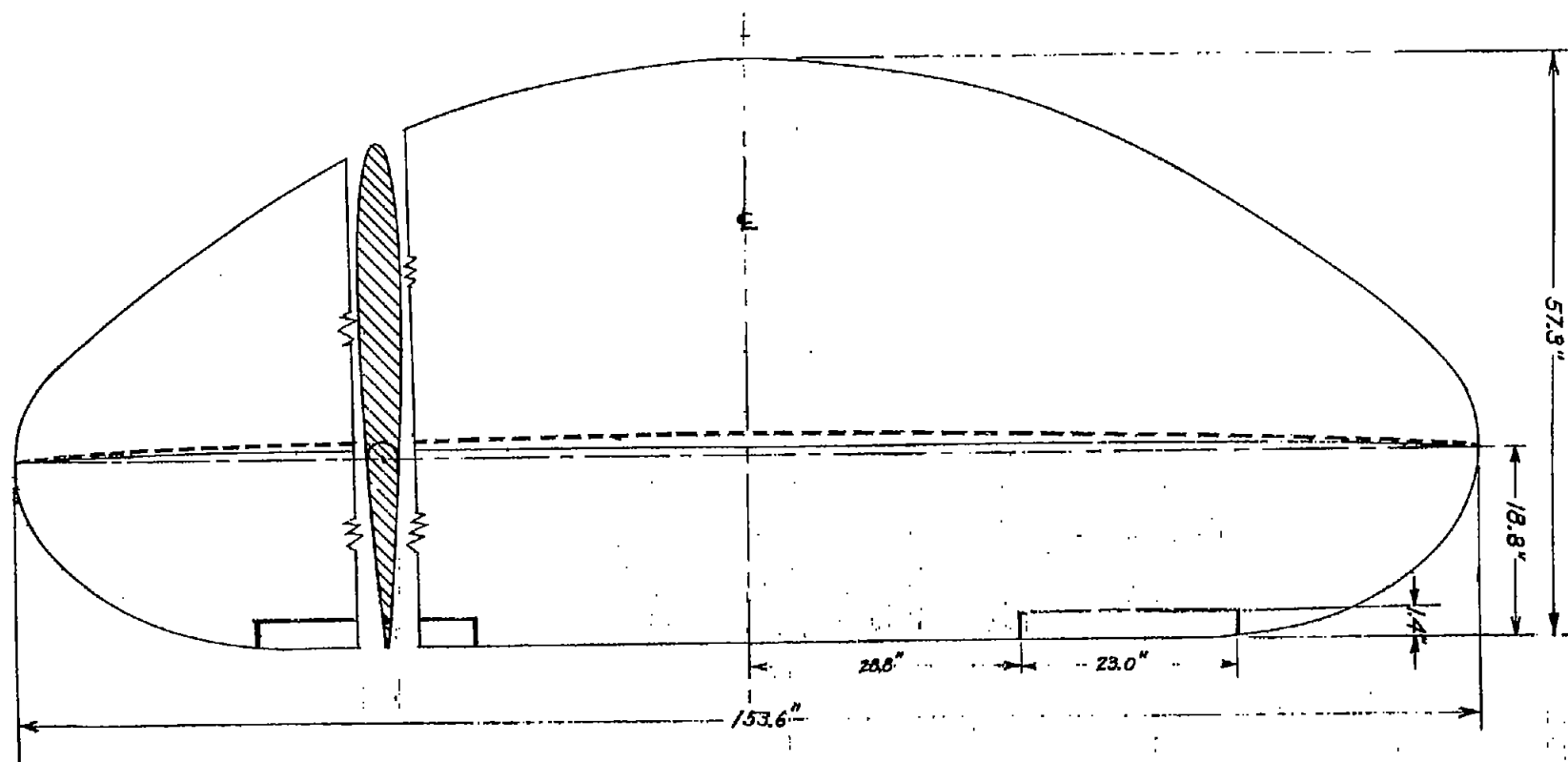


Figure 7.- Tail surface with elliptical airfoil-chord distribution and constant-chord plain flap and tab.